JOURNAL OF APPLIED ELECTROCHEMISTRY **22** (1992) 743–748

Indirect anodic oxidation of anthracene to anthraquinone in a slurry electrolyte system in the presence of both surfactant and redox mediator

T.-C. CHOU, C.-H. CHENG

Department of Chemical Engineering, National Cheng Kung University, Tainan, Taiwan, 701

Received 1 September 1991; revised 4 November 1991

The anodic oxidation of anthracene has been studied in a slurry electrolyte containing both the redox mediator, Mn^{3+}/Mn^{2+}, and surfactant, dodecyl-benzene-sulphonate (DBS). The reaction mechanism, kinetics and the factors which affect the current efficiency of anthraquinone production were explored. Both the experimental results and the theoretical analysis show that the reaction is second order, i.e. first order with respect to Mn^{3+} and DBS, when the concentration of DBS is less than 1.64×10^{-4} M and is first order with respect to Mn^{3+} only when the DBS concentration is larger than 1.64×10^{-4} M. No anthraquinone was found in the absence of DBS. The main factors affecting the current efficiency of the anodic oxidation of anthracene to anthraquinone in the presence of both Mn^{3+}/Mn^{2+} and DBS are H_2SO_4 concentration, current density, anthracene particle size, concentration of DBS and redox mediator as well as temperature. The current efficiency is slightly affected by the concentration of DBS and agitation rate when the concentration of DBS and agitation rate are higher than 1.64×10^{-4} M and 700 r.p.m., respectively.

1. Introduction

The indirect anodic oxidation of organic compounds has been widely investigated [1–10]. Ionic couples such as Ce^{3+}/Ce^{4+}, Mn^{2+}/Mn^{3+}, Co^{2+}/Co^{3+}, Cl^-/ClO^- have been used as mediators or as oxygen carriers. The ions were anodically oxidized from the lower oxidation state to the higher and then reacted with the organic substrates. The chemical reactions of the substrates with the mediators may be carried out *in*-cell or *ex*-cell. In the latter case, the chemical reaction is carried out in a separate vessel and the mediator is recycled back to the electrolytic cell for regeneration. In general, there is a two-phase system for both *in*-cell and *ex*-cell electrochemical oxidation of organic compounds in the presence of redox mediator.

The shuttling or interface mass transfer of redox mediators plays an important role in the anodic oxidation of organic compounds involving two phases [6-10]. The Ce^{3+}/Ce^{4+} and Cl^-/ClO^- ionic redox mediators were used to carry out anodic oxidation of toluene and benzyl alcohol [8], respectively, in a two-phase reaction system and it was found that the interface mass transfer was one of the key steps. The anodic oxidation occurred mainly in the aqueous phase by the transfer of organic substrates from the organic phase to the aqueous phase and the transfer of ionic redox mediators between the aqueous and organic phase was difficult. Usually, the reaction rate of an electro-organic synthesis involving two phases and redox mediators can be significantly improved by increasing the mass transfer of the redox mediator between the organic and aqueous phases.

Recently, phase transfer catalysis has been widely applied to organic synthesis involving organic and aqueous phases [11]. The applications of phase transfer catalysis in electrochemical processes have been discussed by several investigators [8, 11–19]. However, few of these reports are concerned with electrolysis systems in the presence of both phase transfer catalyst and redox mediator [7, 8, 20–23]. In general, the phase transfer catalysts/redox mediators are used in two-phase liquid (aqueous)–liquid (organic) systems. Electrolysis of a solid organic substrate in aqueous solution in the presence of both redox mediator and surfactant or phase transfer catalyst is seldom mentioned.

The indirect anodic oxidation of anthracene in aqueous solution is a typical solid–liquid, or slurry process and has been described by several investigators [24–26]. In this slurry process, in general, the metal ions are anodically oxidized in aqueous solution and form an oxidant which may contact or transfer to the solid substrate by vigorous agitation. However, the kinetics and the parameters affecting the current efficiencies of this slurry electrolysis in the presence of both Mn^{3+}/Mn^{2+} redox mediators and surfactants or phase transfer catalyst are not clear.

The anodic oxidation of anthracene to form anthraquinone in the presence of both Mn^{3+}/Mn^{2+} redox mediator and surfactant (dodecyl-benzene-sulphonate, DBS) or phase transfer catalyst was systematically studied in this work. The particle size of the substrate and the behaviour of the slurry electrolyte system were explored experimentally and theoretically.

0021-891X/92

2. Experimental details

A cylindrical glass reactor 8.5 cm high and 5.5 cm in diameter contained a PbO_2 coated screen as anode, a platinum wire as cathode and a saturated calomel electrode with a Luggin capillary as the reference electrode. The slurry electrolyte and substrate was formed by mixing the desired amount and particle size of anthracene powder and the aqueous solution with a desired concentration of both Mn^{2+} and sulphuric acid. The slurry electrolyte was agitated by a motorized stirrer (EYELA DC-2RT). The d.c. power was supplied by a potentiostat/galvanostat (HOKUTO HA-201).

The electrolysis procedure was as follows. The slurry electrolyte was formed by mixing 1.0 g of the desired particle size, 110 mesh, of anthracene particles with 250 ml of 5.5 M H_2SO_4 aqueous solution which contained the desired concentration of Mn^{2+} and DBS. The whole reactor was immersed in a water bath which was controlled at a desired temperature within ±0.1° C. At the beginning of a run, the stirrer was switched on and the electrolysis was carried out at constant current. During the run, the aqueous solution was sampled periodically and analysed by titration with standard Fe^{2+} solution. At the end of the run, the solid product was washed with distilled water, filtered and dried in an oven. The solid product was dissolved in chloroform and analysed by GC.

3. Results and discussion

3.1. *Effect of agitation*

The mass transfer or shuttling of the redox ion between the anode and the anthracene particle may play an important role in this slurry reaction system. In general, agitation may change both the mass transfer coefficient and the mass transfer interfacial area in a two-phase system. Therefore, the effect of agitation on the current efficiency was experimentally tested. The results reveal that the current efficiency is significantly affected by the mass transfer rate of the redox mediator for almost all particle sizes when the stirring rate is less than 700 rpm as shown in Fig. 1. This indicates that the redox ions transfer rate across the boundary layer depends on the film mass transfer coefficient of the Mn^{3+}/Mn^{2+} redox ions between the anthracene particle and aqueous solution. On increasing the stirring rate from 700 r.p.m. to 800 r.p.m. or more, the current efficiency and the reaction rate do not increase. This indicates that the reaction system is not affected by the mass transfer and reaction control occurs. The stirring rate was maintained at 700 r.p.m. for the following runs to evaluate other factors affecting the current efficiency and kinetics.

3.2. *Effect of concentration of DBS on yield*

As shown in Table 1, increasing the concentration of DBS from 3.56×10^{-5} to 1.64×10^{-4} M increased the yield of anthraquinone from 0.93 to 16.76%. Zero DBS concentration produced zero yield. The results indicate that the redox mediator is more efficiently transferred from the aqueous phase to the anthracene particle and more active sites are created on the anthracene particle when the concentration of DBS increases. On further increase in the DBS concentration to 3.28×10^{-4} M, the increase in the yield of anthraquinone slowed down and reached a constant value as shown in Table 1. This means that the yield or current efficiency may be determined by the anodic oxidation of the Mn^{2+} into Mn^{3+} ion when the concentration of DBS is more than 1.64×10^{-4} M.

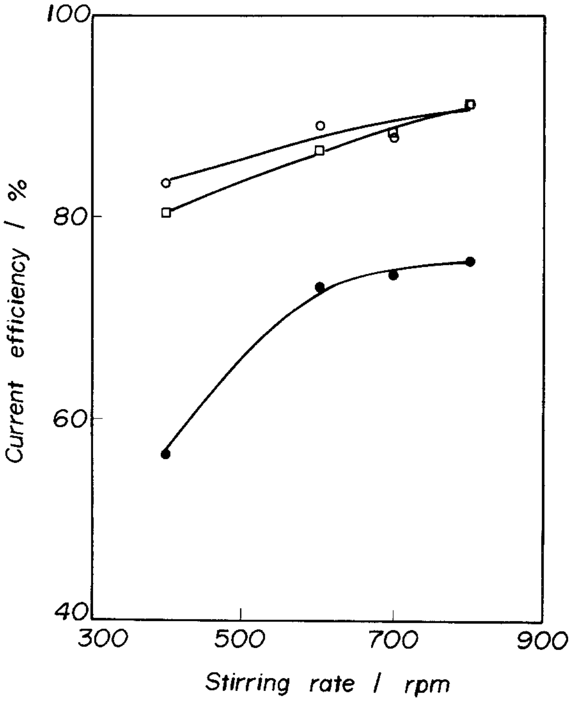

Fig. 1. Effect of stirring rate on the current efficiency. AN: 1.0 g; [Mn^{3+}]: 0.059 M; [DBS]: 1.64×10^{-4} M; temp.: 37° C; volume of solution: 250 ml 5.5 M H_2SO_4. Mesh sizes: (○) 200–400, (□) 100–200, and (●) 80–100.

3.3. *Effect of temperature*

As shown in Table 2, the current efficiency is affected by temperature. At 5.5 M H_2SO_4 increasing the temperature from 34 to 38° C increased the current

Table 1. Effect of concentration of DBS on the yield of AQ in slurry electrolyte system

Concentration of DBS /M	*Weight of AQ* /g	*Yield of AQ* /%
3.56×10^{-5}	2.79×10^{-3}	0.93
4.28×10^{-5}	6.66×10^{-3}	2.22
8.20×10^{-5}	3.18×10^{-2}	10.61
1.64×10^{-4}	5.03×10^{-2}	16.76
3.28×10^{-4}	5.25×10^{-2}	17.50

[Mn^{3+}]: 6.3×10^{-3} M; [H_2SO_4]: 5.5 M; volume of solution: 250 ml; weight of anthracene: 0.3 g; particle size: 100–200 mesh; stirring rate: 700 r.p.m.; reaction time: 15 min.

Table 2. *Effect of temperature on the current efficiency*

Conc. of H_2SO_4 /M	*Temp. /°C*	*Weight of AQ/%*		*C.E. /%*	*Power consumption /kWh kg^{-1} AQ*	*Conversion /%*
		Exp.	*Theor.*			
5.5	34	0.212	0.517	40.98	5.57	18.14
5.5	38	0.317	0.517	61.33	3.48	27.15
5.5	44	0.288	0.517	55.67	4.41	24.65
6.5	38	0.301	0.517	58.13	4.14	25.74
6.5	43	0.377	0.517	72.89	3.19	32.27
6.5	48	0.307	0.517	59.26	3.86	26.24

Anode: PbO_2; cathode: Pt wire; current density: 6.67 mA cm^{-2}; electrolysis time: 2 h; particle size: 80–100 mesh; [Mn^{3+}]: 0.048 M; volume of solution: 250 ml; weight of anthracene: 1.0 g; stirring rate: 800 r.p.m.; surfactant [DBS]: 1.64×10^{-4} M.

efficiency from 40.98 to 61.33% and produced a maximum at 38° C. With further increase in temperature to 44° C, the current efficiency decreased from 61.33 to 55.67%. The effect of temperature on current efficiency at 6.5 M H_2SO_4 is similar to that at 5.5 M. However, the maximum current efficiency is 72.89% and occurs at 43°C in 6.5 M H_2SO_4 rather than 61.33% at 38°C in 5.5 M H_2SO_4 in Table 2. The corresponding minimum specific power consumption as well as the maximum conversion occur at 38° C and 43° C in 5.5 M and 6.5 M H_2SO_4, respectively, as shown in Table 2.

The main steps are the anodic oxidation of Mn^{2+}, the activation of anthracene by DBS and the oxidation of anthracene by the Mn^{3+} ion. The chemical reaction rate significantly increased with the increase in temperature. The solubility of Mn^{2+} decreases sharply with increase in H_2SO_4 and the stability of Mn^{3+} decreases with increasing temperature [6]. These factors may cause the maximum current efficiency to occur at different temperatures for different acid strengths.

3.4. *Effect of H_2SO_4 concentration*

As shown in Table 3, the current efficiency, specific power consumption and conversion were significantly affected by the concentration H_2SO_4. A minimum current efficiency, 58.13%, was obtained at 6.5 M H_2SO_4. The current efficiency is higher, 71.32%, at 38°C in 7.5 M H_2SO_4. The results show that the stability and the solubility of Mn^{3+}/Mn^{2+} redox mediators in aqueous solution depend on the concentration of H_2SO_4.

3.5. *Effect of electrolysis time*

Table 4 shows the effect of the charge passed or electrolysis time on the current efficiency. In general, the current efficiency decreased with electrolysis time for a batch and direct anodic oxidation electrolysis, since the concentration of substrate decreased and the electrolysis side reaction increased. On the other hand, for a batch and indirect electrolysis, the current efficiency increases with electrolysis time. It is necessary to build up the concentration of the oxidizing species of the redox mediator. The substrate in this slurry electrolyte is the anthracene solid particles; the formation of product anthraquinone depends on the reaction of Mn^{3+} ion with anthracene. Initially, the current efficiency is very low. This indicates that the anodically generated Mn^{3+} ion is at too low a concentration to form significant anthraquinone. During the period of 1 to 2 h of electrolysis, the current efficiency increased sharply since the accumulation of Mn^{3+} was sufficiently high for oxidation to proceed.

Further increase in electrolysis time, prdouced an increase in current efficiency to a maximum, 64.35%, at 3 h of electrolysis time and slightly decreased when the electrolysis time was 4 h, as shown in Table 4. The specific power consumption decreased during the first hour of electrolysis and then remained constant while the conversion of anthracene increased with electrolysis time as shown in Table 4.

3.6. *Effect of current density*

The current efficiency decreases when the current density increases. Increasing the current density from 3.67

Table 3. *Effect of concentration of H_2SO_4 on the current efficiency*

Conc. of H_2SO_4 /M	*Weight of AQ/%*		*C.E. /%*	*Power consumption /kWh kg^{-1} AQ*	*Conversion /%*
	Exp.	*Theor.*			
5.5	0.317	0.517	61.33	3.48	27.15
6.5	0.301	0.517	58.13	4.14	25.74
7.5	0.369	0.517	71.32	3.16	31.58

Anode: PbO_2; cathode: Pt wire; current density: 6.67 mA cm^{-2}; electrolysis time: 2 h; particle size: 80–100 mesh; [Mn^{3+}]: 0.048 M; volume of solution: 250 ml; weight of anthracene: 1.0 g; stirring rate: 800 r.p.m.; surfactant [DBS]: 1.64×10^{-4} M; temperature: 38° C.

Table 4. Effect of electrolysis time on the current efficiency

Electrolysis time/h	*Weight of AQ*/%		*C.E.* /%	*Power consumption* /kWh kg^{-1} AQ	*Conversion* /%
	Exp.	*Theor.*			
1.0	0.043	0.259	20.54	14.22	3.67
2.0	0.317	0.517	61.33	3.48	27.15
3.0	0.499	0.776	64.35	3.68	42.74
4.0	0.652	1.035	63.01	3.87	55.79

Anode: PbO_2; cathode: Pt wire; current density: 6.67 mA cm^{-2}; particle size: 80–100 mesh; [Mn^{3+}]: 0.048 M; volume of solution: 250 ml in 5.5 M H_2SO_4; weight of anthracene: 1.0 g; stirring rate: 800 r.p.m.; surfactant [DBS]: 1.64 × 10^{-4} M; temperature: 38° C.

to 10.00 mA cm^{-2} at 38° C, 2 h electrolysis time, 800 r.p.m. stirring rate, 80–100 mesh anthracene, 0.048 M Mn^{2+}, 5.5 M H_2SO_4 and 1.64 × 10^{-4} M DBS, the current efficiency decreased from 64.84 to 55.60%. The specific power consumption increased from 3.64 to 4.57 kWh kg^{-1} AQ and the conversion of anthracene increased from 15.79 to 36.93%, when the current density increased from 3.67 to 10.00 mA cm^{-2} as shown in Table 5. This may be due to the increase in oxygen evolution when the current density increases.

3.7. *Effect of particle size and particle size distribution*

Three different ranges, 80–100, 100–200, 200–400 mesh, anthracene particle size were used as the substrate. The current efficiency increased with decreasing particle size. As shown in Table 6, for 80–100 mesh, the current efficiency was much less than that for 100–200 or 200–400 mesh. The current efficiency increased to 91.20% when the anthracene particle size decreased to 100–200 mesh. Further decreases in the particle size did not cause an increase in the current efficiency and kept the current efficiency at 91.20% as shown in Table 6.

In order to test the particle size distribution change during the electrolysis, two runs were carried out. The blank test was carried out at 38° C, 150 r.p.m., 50–60 mesh particle size of 1 g substrate and 78 min mixing without electrolysis, and the particle size distribution was found to be in the range 300–500 μm. The results revealed that the change of particle size distribution is insignificant if no oxidation reaction takes place. The conditions for electrolysis were the same except that a 6.67 mA cm^{-2} current density was passed. The particle size distribution concentrated in two groups, one in the region of 8 μm and the other near 200 μm. The results indicate that the anthracene particles are broken down when the anthracene is oxidized to form anthraquinone.

3.8. *Kinetics of indirect anodic oxidation of anthracene in slurry electrolyte*

3.8.1. Effect of DBS concentration. Figure 2 and Table 7 show the effect of DBS concentration on the initial reaction rate of anthracene oxidation by Mn^{3+} ion. Figure 2 is the plot of Mn^{3+} ion concentration against time. The concentration of anthracene or the concentration of Mn^{3+} at 1.14 × 10^{-4} M DBS decreased faster than those at 2.85 × 10^{-5} M DBS as shown in Fig. 2. The slopes of the curves of Fig. 2 at the beginning of the runs are the experimental initial reaction rates as shown in Table 7. The logarithmic plot of the initial reaction rate against DBS concentration gave a straight line with a slope 1.15 as shown in Table 7, i.e.

$$R_p \propto [\mathrm{DBS}]^{1.15} \qquad (1)$$

The initial reaction rate is independent of the concentration of DBS when the concentration of DBS is higher than 1.64 × 10^{-4} M.

3.8.2. Effect of Mn^{3+} concentration on the reaction rate. Figure 3 shows the plots of Mn^{3+} concentration against time during the reaction of Mn^{3+} with anthracene. The initial reaction rates can be obtained from the curves in Fig. 3 as shown in Table 8. The logarithmic plot of the initial reaction rate vs. Mn^{3+} concentration resulted in a straight line of slope 0.92 as shown in Table 8. The results can be expressed as

$$R_p \propto [\mathrm{Mn}^{3+}]^{0.92} \qquad (2)$$

Table 5. Effect of current density on the current efficiency

C.D. /mA cm^{-2}	*Weight of AQ*/%		*C.E.* /%	*Power consumption* /kWh kg^{-1} AQ	*Conversion* /%
	Exp.	*Theor.*			
3.67	0.185	0.285	64.84	3.42	15.79
6.67	0.317	0.517	61.33	3.48	27.15
10.00	0.431	0.776	55.60	4.57	36.93

Anode: PbO_2; cathode: Pt wire; particle size: 80–100 mesh; [Mn^{3+}]: 0.048 M; volume of solution: 250 ml in 5.5 M H_2SO_4; weight of anthracene: 1.0 g; stirring rate: 800 r.p.m.; surfactant [DBS]: 1.64 × 10^{-4} M; temperature: 38° C; electrolysis time: 2 h.

Table 6. Effect of particle size on the current efficiency

Particle size /mesh	Exp. weight of AQ /g	Theor. weight of AQ /g	C.E. /%
80–100	0.386	0.511	75.4
100–200	0.466	0.511	91.2
200–400	0.466	0.511	91.2

[Mn^{3+}]: 0.059 M; volume of solution: 250 ml 5.5 M H_2SO_4; weight of anthracene: 1.0 g; stirring rate: 700 r.p.m.; reaction time: 55 min; temperature: 37° C; surfactant [DBS]: 1.64×10^{-4} M.

Table 7. Effect of concentration of DBS on the reaction rate

Conc. of DBS /M	Ln [DBS] /M	R_p /M min^{-1}	Ln (R_p) /M min^{-1}
2.85×10^{-5}	−10.47	9.17×10^{-6}	−11.60
5.70×10^{-5}	−9.77	1.83×10^{-5}	−10.91
8.55×10^{-5}	−9.37	8.52×10^{-5}	−10.40
1.14×10^{-4}	−9.08	4.54×10^{-5}	−10.00

[Mn^{3+}]: 4.92×10^{-3} M; volume of solution: 250 ml 5.5 M H_2SO_4; weight of anthracene: 0.3 g; stirring rate: 700 r.p.m.; temperature: 37° C; particle size: 100–200 mesh.

On the basis of Equations 1 and 2 this gives:

(i) for DBS concentration less than 1.64×10^{-4} M

$$R_p = k[Mn^{3+}]^{0.92}[DBS]^{1.15} \qquad (3)$$

(ii) for DBS concentration larger than 1.64×10^{-4} M,

$$R_p = k'[Mn^{3+}]^{0.92} \qquad (4)$$

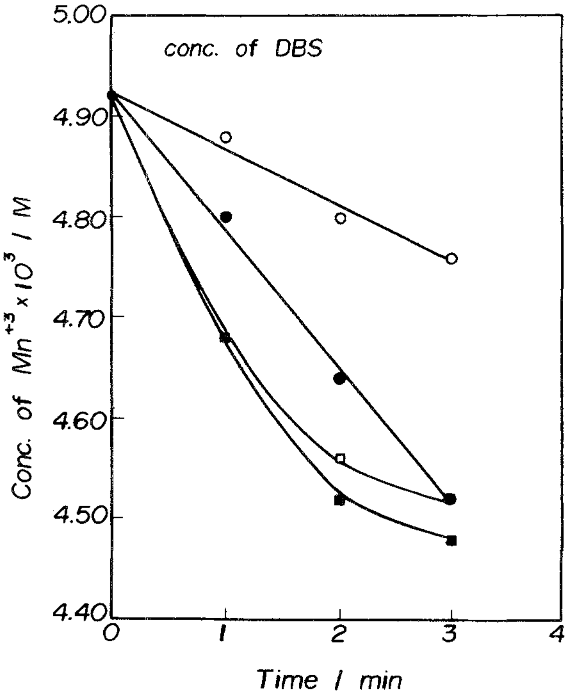

Fig. 2. Concentration of Mn^{3+} against time in solid-aqueous-phase system. AN: 0.3 g; [DBS]: 4.92×10^{-3} M; particle size: 100–200 mesh; stirring rate: 700 r.p.m.; volume of solution: 250 ml 5.5 M H_2SO_4; temp.: 37° C. DBS concentrations: (○) 2.85×10^{-5}, (●) 5.70×10^{-5}, (□) 8.55×10^{-5}, and (■) 1.14×10^{-4} M.

Table 8. Effect of concentration of Mn^{3+} on the reaction rate

Conc. of Mn^{3+} /M	Ln [Mn^{3+}] /M	$R_p \times 10^4$ /M min^{-1}	Ln (R_p) /M min^{-1}
3.77×10^{-3}	−5.58	1.0	−9.21
1.19×10^{-2}	−4.43	3.2	−8.04
2.26×10^{-2}	−3.79	4.0	−7.82
4.33×10^{-2}	−3.14	10.7	−6.84

Volume of solution: 250 ml 5.5 M H_2SO_4; weight of anthracene: 0.3 g; stirring rate: 700 r.p.m.; temperature: 37° C; surfactant [DBS]: 1.64×10^{-4} M; particle size: 100–200 mesh.

Table 9. Effect of temperature on the rate constant in slurry electrolyte system

T /K	1/T /K^{-1}	k /min^{-1} g^{-1}	Ln (k) /min^{-1} g^{-1}
300	3.33	1.69×10^{-2}	−4.08
305	3.28	2.07×10^{-2}	−3.88
310	3.23	6.14×10^{-2}	−2.79
315	3.17	1.01×10^{-1}	−2.29

Volume of solution: 250 ml 5.5 M H_2SO_4; weight of anthracene: 0.3 g; stirring rate: 700 r.p.m.; surfactant [DBS]: 1.64×10^{-4} M; particle size: 100–200 mesh.

3.8.3. Effect of temperature. The effect of temperature on the rate constant is shown in Table 9. The Arrhenius plot of the rate constant against the reciprocal of absolute temperature gave a straight line of slope −12.16 as shown in Table 9. This corresponds to an activation energy of 24.16 kcal mol^{-1}. This suggests that the chemical reaction is the rate controlling step.

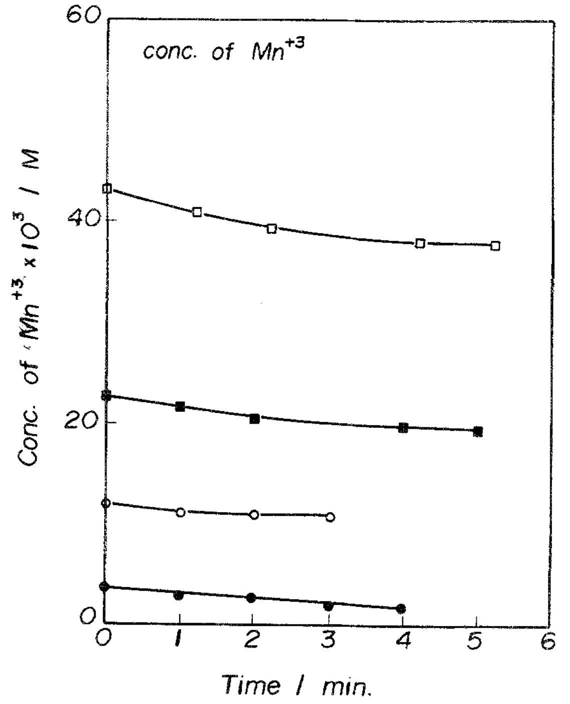

Fig. 3. Concentration of Mn^{3+} against time in solid-aqueous-phase system. AN: 0.3 g; [DBS]: 1.64×10^{-4} M; particle size: 100–200 mesh; stirring rate: 700 r.p.m.; volume of solution: 250 ml 5.5 M H_2SO_4; temp.: 37° C. Mn^{3+} concentrations: (□) 4.33×10^{-2}, (■) 2.26×10^{-2}, (○) 1.19×10^{-2}, and (●) 3.77×10^{-3} M.

4. Conclusions

The results indicate that the surfactant plays an important role in the electrolysis of solid anthracene. The DBS makes the lipophilic anthracene particle active for the Mn^{3+} ion which is hydrophilic. The reaction rate is second order at lower DBS concentration and first order at higher DBS concentration.

The main factors affecting the current efficiency are the H_2SO_4 concentration, current density, anthracene particle size, DBS and redox mediator concentration and temperature. On the other hand, the current efficiency is only slightly affected by the DBS concentration and agitation rate when the DBS concentration and the agitation rate are higher than 1.64×10^{-4} M and 700 r.p.m., respectively.

Acknowledgement

The support of the National Science Council of the Republic of China is acknowledged.

References

[1] K. Kramer, P. M. Robertson and N. Ibl, *J. Appl. Electrochem.* **100** (1980) 29.
[2] H. Wendt and H. Schneider, *ibid.* **16** (1986) 134.
[3] I. M. Dalrymple and J. P. Millington, *ibid.* **16** (1986) 885.
[4] J. J. Jow, A. C. Lee and T. C. Chou, *ibid.* **17** (1987) 753.
[5] Ch. Comminellis and E. Plattner, *ibid.* **9** (1979) 593.
[6] J. J. Jow and T. C. Chou, *ibid.* **18** (1988) 298.
[7] J. S. Do and T. C. Chou, *ibid.* **19** (1989) 922.
[8] *Idem, ibid.* **20** (1990) 978.
[9] U.S. Patent Nos. 4212710 and 4582942.
[10] J. S. Do and T. C. Chou, *I & EC Research* **29** (1990) 1095.
[11] C. M. Starks, 'Phase Transfer Catalysis', ACS Symposium Series (1987), p.1.
[12] S. R. Ellis, D. Pletcher, P. Gough and S. R. Korn, *J. Appl. Electrochem.* **12** (1982) 687.
[13] S. R. Ellis, D. Pletcher, P. H. Gramlen and K. P. Healy, *ibid.* **12** (1982) 693.
[14] M. Fleischmann, C. L. K. Tennakoon, H. A. Bampfield and P. J. Williams, *ibid.* **13** (1983) 593.
[15] M. Fleischmann, C. L. K. Tennakoon, P. Gough, J. H. Steven and S. R. Korn, *ibid.* **13** (1983) 603.
[16] S. R. Ellis, D. Pletcher, W. N. Brooks and K. P. Healy, *ibid.* **13** (1983) 735.
[17] S. R. Forsyth, D. Pletcher and K. P. Healy, *ibid.* **17** (1987) 905.
[18] E. Laurent, G. Rauniyar and M. Thomalla, *ibid.* **14** (1984) 741.
[19] *Idem, ibid.* **15** (1985) 121.
[20] D. Pletcher and N. R. Tomov, *ibid.* **2** (1977) 50.
[21] R. E. W. Janson and N. R. Tomov, *ibid.* **10** (1980) 583.
[22] L. C. Jiang and D. Pletcher, *J. Electroanal. Chem.* **152** (1983) 157.
[23] *Idem, ibid.* **33** (1988) 509.
[24] K. Shirai and K. Sugino, *Denki Kaguku* **25** (1957) 284.
[25] I. Nishiguchi, Recent Progress of Industrial Electroorganic Synthesis, The Ind. International Symposium on Electrochemistry (1985), p.285.
[26] R. L. Clarke and A. R. Wasson, *AIChE Symp. Series* **79** (1983) 85.
[27] J. J. Ziolkowski and T. B. Szymanska, *J. Mol. Cat.* **5** (1979) 341.
[28] C. K. Das and N. S. Das, *J. Chem. Tech. Biotech.* **39** (1987) 183.